Highly Conductive and Ultrastretchable Electric Circuits from Covered Yarns and Silver Nanowires

Yin Cheng, Ranran Wang,* Jing Sun,* and Lian Gao

State Key Laboratory of High Performance Ceramics and Superfine Microstructure, Shanghai Institute of Ceramics, Chinese Academy of Sciences, Shanghai 200050, China

ABSTRACT

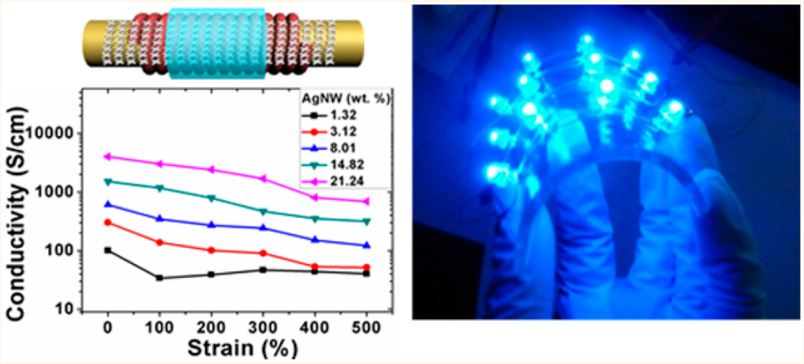

Stretchable electronics, as a promising research frontier, has achieved progress in a variety of sophisticated applications. The realization of stretchable electronics frequently involves the demand for a stretchable conductor as an electrical circuit. However, it still remains a challenge to fabricate high-performance (working strain exceeding 200%) stretchable conductors. Here, we present for the first time a facile, cost-effective, and scalable method for manufacturing ultrastretchable composite fibers with a "twining spring" configuration: cotton fibers twining spirally around a polyurethane fiber. The composite fiber possesses a high conductivity up to 4018 S/cm, which remains as high as 688 S/cm at 500% tensile strain. In addition, the conductivity of the composite fiber (initial conductivity of 4018 S/cm) remains perfectly stable after 1000 bending events and levels off at 183 S/cm after 1000 cyclic stretching events of 200% strain. Stretchable LED arrays are integrated efficiently utilizing the composite fibers as a stretchable electric wiring system, demonstrating the potential applications in large-area stretchable electronics. The biocompatibility of the composite fiber is verified, opening up its prospects in the field of implantable devices. Our fabrication strategy is also versatile for the preparation of other specially functionalized composite fibers with superb stretchability.

KEYWORDS: silver nanowires · composite fibers · twining spring configuration · stretchable electric circuits · implantable

Stretchable electronics, as an emerging and fascinating research scope in the last ~15 years, has motivated intensive efforts from materials scientists and engineers.[1,2] This new class of electronics has gained achievements and opened up a wide variety of sophisticated application fields, including stretchable displays,[3,4] skin-like sensors,[5,6] strain/pressure sensors for human-motion detection,[7−9] electronic eye cameras,[10] stretchable energy-related devices,[11,12] and implantable devices for human health monitoring.[13] One of the most formidable challenges involved to realize these devices, however, is the development of stretchable conductors that are capable of retaining high conductivity even under severe deformation, such as bending and high-strain (>50%) stretching. To overcome this hurdle, researchers have come up with various strategies. One approach exploits the incorporation of conductive filler materials, such as metal nanoparticles,[14] graphite,[15] carbon nanotubes (CNTs),[16,17] and conducting polymers,[18] into a rubbery polymer matrix through blending. Takao Someya dispersed single-walled carbon nanotubes (SWCNTs) uniformly into a vinylidene fluoride–hexafluoropropylene copolymer matrix to

* Address correspondence to wangranran@mail.sic.ac.cn, jingsun@mail.sic.ac.cn.

Received for review December 12, 2014 and accepted March 25, 2015.

Published online March 25, 2015
10.1021/nn5070937

form a composite film as a stretchable conductor.[16] This elastic conductor exhibited an initial conductivity of 57 S/cm and could be uniaxially stretched up to 134% with a final conductivity of 6 S/cm. Seunghyun Baik reported conductive and stretchable hybrid composites composed of micrometer-sized silver flakes and multiwalled carbon nanotubes (MWCNTs) decorated with self-assembled silver nanoparticles.[17] The maximum conductivity of the silver-CNT stretchable conductor was as high as 5710 S/cm at 0% strain. However, the conductivity unfavorably decreased dramatically to 20 S/cm at 140% strain, at which point the film ruptured. There existed a limit to this strategy, where incorporation of high concentrations of conductive fillers such as CNTs into the polymer matrix increases the stiffness and decreases the stretchability of the resultant composite. Another route takes advantage of already existing three-dimensional porous and conducting networks through infiltrating a liquid polymer into the network, including CNT forest-based elastomeric conductive composites,[19] SWCNT aerogel-based elastic conductors,[20] and three-dimensional graphene network (grown by chemical vapor deposition) based composite conductors.[21] The high performance of this sort of stretchable conductors is usually confined within a moderate strain (<100%) to maintain the integrity of the conducting networks. Besides the above two categories, the most frequently used strategy is to construct special structural configurations capable of restoring prestrain, such as net-shaped films, in-plane wavy structures, and out-of-plane buckled structures.[12,13,22−35] This strategy enables relatively stable electrical performance within the prestrain range when subjected to deformation, although the construction of such configurations is usually time-consuming and also hard to scale up.

Until now, it still remains a challenging task to develop a facile, cost-effective, and scalable way to fabricate a high-strain elastic conductor with stable high conductivity. Herein, we developed for the first time a manufacturing approach for a highly conductive, flexible, and ultrastretchable composite fiber based on an artfully designed "twining spring" architecture. The composite fiber comprises a selected double-covered yarn (DCY), serving as an elastic scaffold, silver nanowires (AgNWs) as the conducting component, and a poly(dimethylsiloxane) (PDMS) encapsulation as a strengthening and protective layer. The conductivity of the conductive elastic fiber reaches up to 4018 S/cm at 0% strain and remains as high as 688 S/cm at 500% strain, rendering our conducting fiber highly competitive among the nanomaterial-based stretchable conductors. The composite fiber also possesses superb cyclic performance, with conductivity leveling off at 183 S/cm after 1000 stretching events of 200% strain. Its potential application in large-area stretchable electronics is demonstrated through integrating LED arrays on a transparent, bendable, and stretchable substrate with the composite fibers acting as stretchable interconnects. At last, the biocompatibility of the composite fiber is validated, thus opening up its prospects in the field of implantable devices.

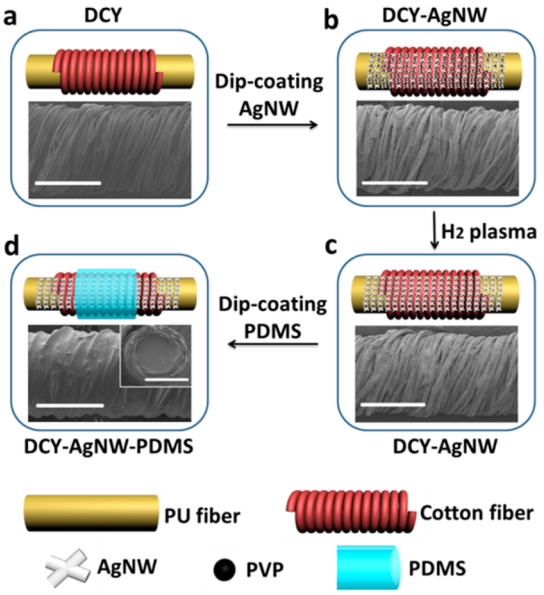

Figure 1. Schematic illustration of the fabrication process of the composite fiber. (a) Structural representation and SEM image of the DCY. For simplicity and clarity, only one CY was demonstrated in the structural drawing. (b) Structural representation and SEM image of DCY-AgNW before H_2 plasma treatment. (c) Structural representation and SEM image of DCY-AgNW after H_2 plasma treatment. (d) Structural representation and SEM images of DCY-AgNW-PDMS. The inset SEM image shows the cross-sectional structure. The PDMS infiltrated the whole CY layer. Scale bar for all: 500 um. The DCY, DCY-AgNW, and DCY-AgNW-PDMS all have diameters of ~650 um.

RESULTS AND DISCUSSION

Figure 1 presents a schematic illustration of the preparation of the conductive and stretchable composite fiber (detailed procedures are described in the Methods). The DCY, a kind of cotton/Spandex yarn, is inexpensive and widely used in the textile industry. Typically, the polyurethane (PU) monofilament served as the core fiber and was tightly wrapped by two cotton yarns (CYs) in opposite directions like compressed springs (Figure 1a, Figure S1 in the Supporting Information). Both CYs are composed of numerous cotton fibers (CFs). This kind of DCY is carefully selected for the reason that it combines perfectly the superb elasticity provided by the PU fiber, increased specific surface area, and hygroscopicity guaranteed by the two CYs, which is key to the efficient "dyeing" of AgNWs (Figure S2, Supporting Information). In addition, the unique spiral configuration of the CYs preserves the extremely large prestrain (>500%), suggesting that no actual elongation of the CYs takes place when the DCY is stretched. A dip-coating method was employed to intimately coat AgNWs onto the

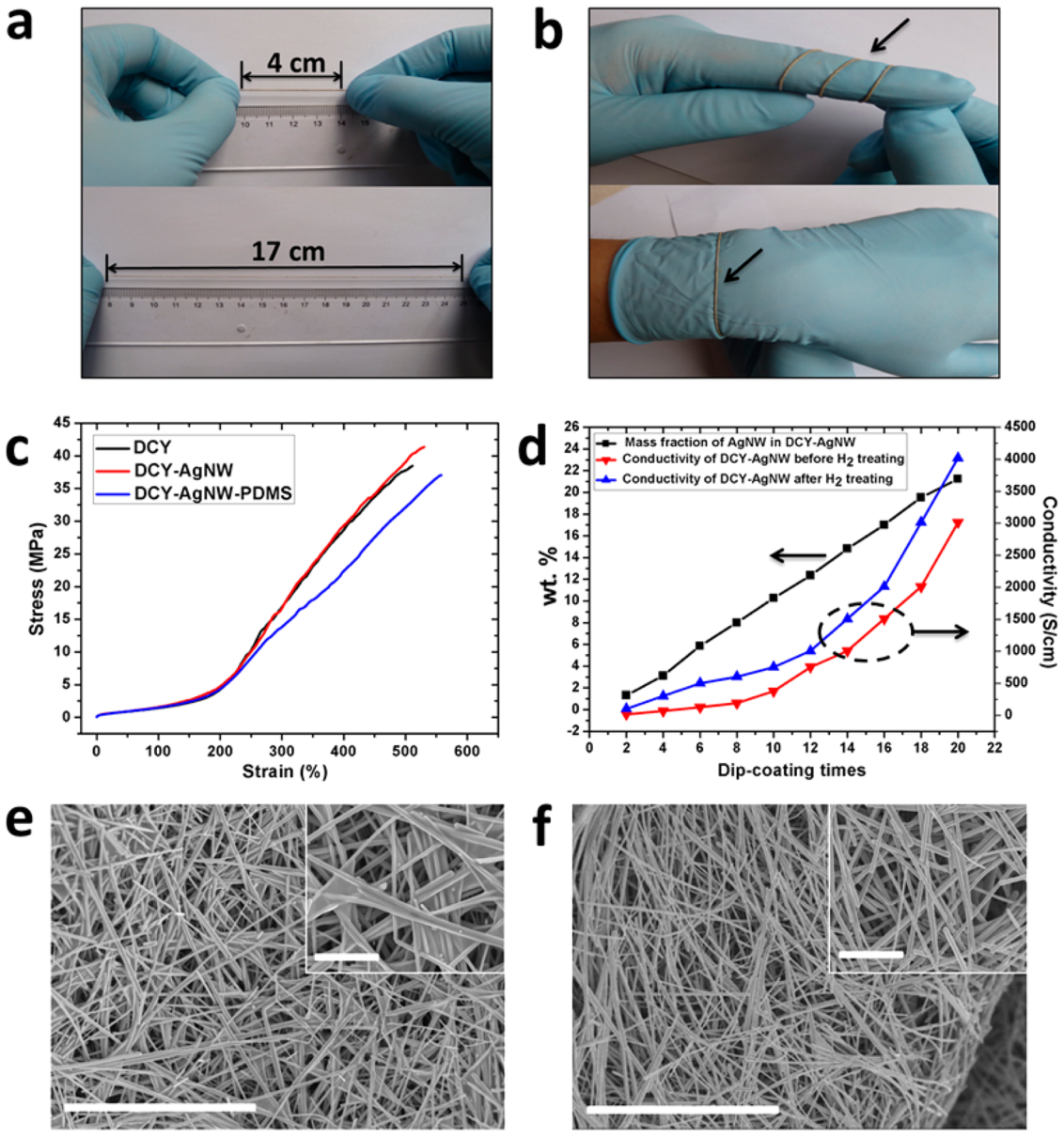

Figure 2. Mechanical properties of DCY/DCY-AgNW-PDMS and effects of dip-coating times and H_2 plasma treatment on the electrical conductivity of DCY-AgNW. (a) A fabricated composite fiber of 4 cm was stretched to 17 cm by hand. Larger strain could be obtained with the help of a universal testing machine. (b) The flexible composite fiber conformed well to a human finger and wrist, demonstrating its possible utilization in wearable electronics. (c) Typical stress−strain curves of DCY, DCY-AgNW, and DCY-AgNW-PDMS. (d) Variation of the mass fraction of AgNW in DCY-AgNW and the conductivity of the DCY-AgNW before and after H_2 plasma treatment along with dip-coating times of AgNWs. (e) SEM image of the AgNW network on a CF surface before H_2 plasma treatment. The inset is the magnified SEM image for a localized position. (f) SEM image of the AgNW network on the CF surface after H_2 plasma treatment. The inset is the magnified SEM image for a localized position. Scale bar of the main SEM images in (e) and (f) is 10 μm. Scale bar of the inset images in (e) and (f) is 2 μm.

surface of the CFs of the DCY (Figure 1b), resulting in a DCY covered with AgNWs (DCY-AgNW). The dip-coating process is similar to the "dyeing" process in the textile industry, which has been utilized for the fabrication of electronic textiles.[11,36−39] Subsequent to the "dyeing" of AgNWs, for the sake of higher conductivity, the DCY-AgNW was then treated with H_2 plasma to remove the polyvinylpyrrolidone (PVP) accompanying the AgNW as a dispersing agent in solution (Figure 1c, discussed later). Finally, the DCY-AgNW was encapsulated by a thin PDMS layer *via* dip-coating (Figure 1d). The PDMS played roles in strengthening the structure mechanically and anchoring AgNWs onto the surface of the CFs. No measurable damage of conductivity was brought about by the coating of PDMS. The CFs twining around the PU fiber, acting like a "twining spring", is key to the outstanding performance of the composite fiber. The as-prepared composite fiber is highly elastic (Figure 2a) and can conform well to arbitrary curvilinear surfaces, including human body parts, such as fingers and wrists (Figure 2b), suggesting its possible application in wearable electronics. As a

consequence of the chemical stability of its components, the electrical performance of the composite fiber showed no deterioration over a long span of time, at least for 6 months (Figure S3, Supporting Information). The mechanical properties were evaluated using tensile stress *versus* strain measurements (Figure 2c). The DCY, DCY-AgNW, and DCY-AgNW-PDMS ruptured at a strain above 500% (510%, 530%, and 560%, respectively). The calculated elastic moduli for DCY, DCY-AgNW, and DCY-AgNW-PDMS were 12.06, 13.64, and 10.1 MPa, respectively. We speculated that the coating of AgNW onto the surface of CFs hardened the composite fiber surface, which increased the elastic modulus. After PDMS coating, the curing process (80 °C, 4 h) softened the PU fiber, thus decreasing the elastic modulus. Note that the rupture strain here referred to the failure strain of the PU fiber, as the CYs could extend much longer.

The solution dip-coating method adopted here gives us not only the advantage of mass manufacturing but also the feasibility to tune the conductivity of the composite fiber with ease by controlling the density of AgNWs coated onto the CYs through varying the dip-coating times of the AgNWs. Figure 2d illustrates the dependence of the AgNW mass fraction in DCY-AgNWs and the conductivity of the composite fiber on the number of dip-coating times. As the dip-coating times increase from 2 to 20, the mass fraction of AgNW in DCY-AgNW increases almost linearly from 1.32% to 21.24% and the AgNW network on the surface of the DCY becomes thicker (Figure S4, Supporting Information). What is more, the gaps between the adjacent CYs are bridged by a continuous AgNW network especially when high concentrations of AgNW are used (Figure S4f, Supporting Information). The electrical conductivity of DCY-AgNW is measured before and after the H_2 plasma treatment. Within the initial 10 dip-coating times, the conductivity of DCY-AgNW before H_2 plasma treatment ascends slowly from 15 S/cm (2 dip-coatings) to 376 S/cm (10 dip-coatings) and then soars exponentially to 3013 S/cm at 20 dip-coating events. After H_2 plasma treatment, clearly the conductivity is promoted to, correspondingly, 100 S/cm at 2 dip-coating events, 753 S/cm at 10 events, and 4018 S/cm at 20 events. The SEM images (Figure 2e,f, Figure S5) compare the AgNW networks on a single CF before and after H_2 plasma treatment. Before the treatment, the PVP aggregates at the junction positions of the AgNW network (Figure 2e). After treatment, most of the residual PVP is effectively gotten rid of by the reduction of H_2 plasma (although not completely; FTIR results in Figure S5g), resulting in a relatively clean AgNW network compared with before (Figure 2f). Conceivably, this contributes to far more intimate contact at the junctions of AgNWs, accounting for the remarkable promotion of conductivity. The improvement of electrical conductivity by virtue of H_2 plasma treatment demonstrates a novel and valid approach to promoting the performance of devices based on metallic nanowires involving undesired polymer residues.[40,41]

The key to realizing stretchable electronics is the simultaneous incorporation of excellent mechanical robustness and relatively stable electronic performance. The effect of imposed severe deformation, such as stretching and bending, on the electrical conductivity of DCY-AgNW-PDMS is systematically investigated here. Figure 3a records the conductivity of DCY-AgNW-PDMS of different AgNW mass fractions during their being stretched uniaxially up to a strain of 500%. The five samples with varying AgNW mass fraction all went through a gradual decline of conductivity along with the strain up to 500%. For a sample with 21.24 wt % AgNW, the conductivity varied from 4018 to 688 S/cm as the strain increased from 0% to 500%, 603 to 120 S/cm for 8.01 wt %, and 100 to 40 S/cm for 1.32 wt %. The samples outperformed the vast majority of nanomaterial-based stretchable conductors to date. A nanocomposite fabricated from CNT and silver flakes as a stretchable conductor showed a conductivity degradation from 5710 S/cm to 20 S/cm as the strain rose from 0% to 140% (rupture strain).[17] Another work reported a conductive composite mat of silver nanoparticles and rubber fiber gained a high conductivity of 5400 S/cm, and the conductivity dropped to 610 S/cm at a strain of 140% (larger strain caused irreversible damage to conductivity).[42] Yu *et al.* fabricated a stretchable conductor (conductivity of up to ca. 10.25 S/cm) based on a polyurethane sponge and AgNW, which exhibited a resistance increase of 160% at the final strain of 100%.[43] We here propose that the capability of stretchable conductors to maintain the conductivity after being stretched could be evaluated by the figure of merit $(-\Delta\sigma/\sigma_o)/\varepsilon$, where σ_o is the initial conductivity and $\Delta\sigma$ is the variation of conductivity after being stretched to a strain of ε. Clearly, the smaller the figure of merit, the higher the capability for the stretchable conductor to preserve its conductivity. The figures of merit for the above-mentioned cases are 0.712 at a strain of 140%[17] and 0.634 at a strain of 140%,[42] respectively. In our work, the figures of merit for the composite conducting fiber are 0.251, 0.199, 0.193, 0.2, and 0.166 at strains of 100%, 200%, 300%, 400%, and 500%, respectively, indicating the superior stability of conductivity during the deformation.

To understand the conductivity degradation, we traced the microstructure variation of DCY, DCY-AgNW, and DCY-AgNW-PDMS during the stretching from a strain of 0% to 400% and releasing back to 0% (Figure 3b; Figures S6 and S7 in the Supporting Information). Figure 3b demonstrates the typical microstructure morphology of a composite fiber at different stretching stages. The investigated composite fiber here and in the later part all had a AgNW mass fraction of 21.24 wt %, unless otherwise specified.

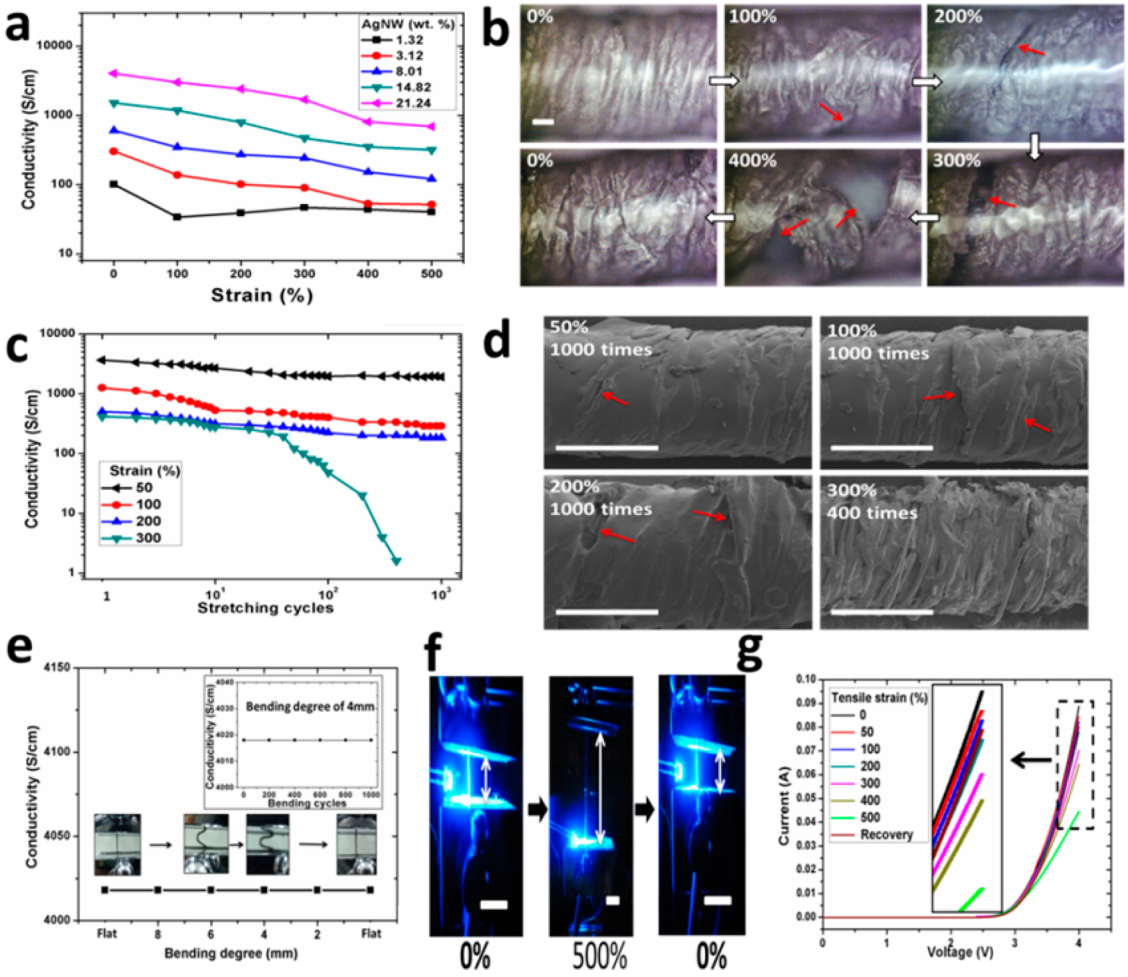

Figure 3. Electrical properties of DCY-AgNW-PDMS under mechanical deformation (stretching/bending) and its application in a LED circuit. (a) Variation of electrical conductivity of DCY-AgNW-PDMS with different AgNW mass fractions *versus* the tensile strain up to 500%. (b) Optical microscopic images of typical microstructure morphology of DCY-AgNW-PDMS at different stretching stages from strains of 0% to 400% and back to 0%. Scale bar (for all strain stages): 100 um. (c) Conductivity of DCY-AgNW-PDMS (4018 S/cm originally) after increasing stretching times at strains of 50%, 100%, 200%, and 300%, respectively. (d) SEM images of DCY-AgNW-PDMS after the cyclic stretching test at strains of 50%, 100%, 200%, and 300%, respectively. The red arrows mark the PDMS gaps in between neighboring CFs caused by cyclic stretching. Scale bar: 500 um. (e) Conductivity of DCY-AgNW-PDMS *versus* the bending degree from flat to 2 mm and back to flat. For convenience, the distance between the two ends of the bent fiber was taken as the assessment of the degree of bending. The photographs are the composite fiber bent at varying bending degree, from flat to 6 mm, to 4 mm, and back to flat. The inset is the cyclic bending test of DCY-Ag-PDMS at a bending degree of 4 mm. (f) Photographs of an LED integrated by DCY-AgNW-PDMS at 4 V, from a strain of 0% (10 mm) to 500% (60 mm) and back to 0% (10 mm). Scale bar: 10 mm. To obtain a panoramic view, the second photograph was taken from a farther distance than the first and third photographs. (g) Current–voltage characteristics of an LED measured at different stretching stages from a strain of 0% to 500% and back to 0%.

As the composite fiber was stretched, the highly elastic PU fiber elongated. At the same time, the spiral CYs twining around the PU fiber axis went through two changes: On one hand, the winding angle of the CYs increased; on the other hand, gaps between CYs emerged and broadened through the stretching (as seen in Figures S6 and S7, Supporting Information). Both the two changes allowed the DCY to experience large strains without actually stretching the CFs. Consequently the AgNW network confined on the surface of the CFs went through little damage during stretching, contributing to a stable conducting path along the CFs. Inevitably, however, the elongation of the composite fiber led to gaps in between the CYs (Figures S6 and S7, Supporting Information), resulting in detaching of the neighboring CFs at the gap position (marked by red arrows in Figure 3b), which consequently disrupted the connection bridged across adjacent CFs by AgNWs (Figure S4f, Supporting Information). The above analysis explains well the high conductivity of the composite fiber and the moderate degradation along with stretching. Also note that the microstructure of DCY-AgNW-PDMS almost reverted to the initial state after being released to a strain of 0% again.

We further undertook a cyclic stretching test of the conductive composite fiber so as to evaluate the stability of the electrical property, which was a crucial

factor from the viewpoint of practical applications. Figure 3c illustrates the conductivity of DCY-AgNW-PDMS (4018 S/cm originally) after cyclic stretching at strains of 50%, 100%, 200%, and 300%, respectively. From the results, for the testing of 50%, 100%, and 200%, the conductivity of DCY-AgNW-PDMS underwent a decrease within the initial ~100 stretching events and then leveled off at conductivities of 1913, 287, and 183 S/cm, correspondingly, even up to 1000 stretching events. For the testing of 300%, the conductivity diminished as the cycling time increased and fell to 1.6 S/cm after 400 times. In fact, the conductivity of the composite fiber was still as high as 48 S/cm even after 100 cyclic stretching events of 300% strain, which was an extremely rigorous test. Also particularly worth mentioning is that the maximal strain for the cyclic stretching test in our study significantly exceeded the standards for other nanomaterial-based stretchable conductors, such as a maximal testing strain for cyclic stretching of 20−50%,[13,17,21,24,27,30,43,44] 60−100%,[19,20,29,31,45] and 110−150%.[16,34,42] This undoubtedly makes our composite fiber a superior candidate for stretchable conductors, especially in high-demand applications involving large (>150%) strain deformation. In order to unravel the mechanism underlying the outstanding performance under cyclic stretching, the morphology of composite fibers after the cyclic stretching test was characterized by SEM, as shown in Figure 3d. The composite fiber was completely encapsulated within a PDMS layer (Figure 1d) after the dip-coating and curing of PDMS. As the composite fiber was stretched, the neighboring CFs detached from each other (discussed above), resulting in cracks in the PDMS in between neighboring CFs. The cracks grew into gaps in the PDMS layer under cyclic stretching (marked by red arrows in Figure 3d). Nevertheless, the PDMS around the surface of the CFs stayed intact favorably during cyclic stretching at strains of 50%, 100%, and 200%. As a consequence, the conducting path along the CF was protected, ensuring relatively stable conductivity even under cyclic stretching up to 200% strain. However, as seen in Figure 3d, a large number of stretching events at a strain of 300% destroyed the structure of DCY-AgNW-PDMS. Peeling off of the PDMS layer from the CF surface occurred after multiple high-strain stretching events, thus disrupting the AgNW network protected under the polymer layer initially, which accounted for the deterioration of electrical conductivity of DCY-AgNW-PDMS under cyclic stretching at a strain of 300%. As a comparison, the cyclic stretching test was also carried out on DCY-AgNW. However, obvious flaking off of AgNWs took place when stretched to a strain above 100% (Figure S7, Supporting Information), which undoubtedly rendered the DCY-AgNW more susceptible to conductivity deterioration (Figure S8, Supporting Information). The comparison results proved the effective and necessary protection supplied by PDMS.

The effect of bending on the electrical conductivity of the composite fiber was investigated. A 10 mm fiber was bent from flat to a bending degree of 2 mm gradually and then back to flat. Figure 3e clearly indicates that the conductivity of the composite fiber remained constant even when bent to a bending degree of 2 mm and straightened to flat. Further cyclic bending testing at a bending degree of 4 mm suggested that the conductivity of the composite fiber remained perfectly stable even after 1000 bending events, without any sign of degradation (Figure 3e inset).

The electrical performance of the composite fiber was visually demonstrated *via* illuminating a light-emitting diode (LED) as stretchable electric wiring. The LED stayed operational at a voltage of 4 V when stretched from a strain of 0% up to 500% and then back to 0%. As seen in Figure 3f, no conspicuous degradation of brightness was noticed during the stretching and releasing. The current−voltage response curve of the LED was examined during the stretching up to a strain of 500% and releasing back to 0% (Figure 3g). The LED was turned on when the applied voltage was greater than 2.8 V due to the energy band gap of the LED. The current decreased as the electric circuit was stretched to a larger strain, and the current−voltage characteristics were partly recovered when the strain was released. In addition, a cyclic stretching/releasing test at strains of 50%, 100%, and 150% continuously was implemented using the composite fiber as circuit wiring for an LED (Supplementary Movie 1).

Large-area stretchable electronics is one of the most cutting-edge and yet extremely challenging research fields currently. Nevertheless only limited progress has been made through exploiting the construction of stretchable circuitry with a "spring within a spring" configuration, which usually involved time-consuming, costly, and complex technological processes such as electron beam evaporation, electroplating, soldering, photolithography, and chemical etching.[12,13] Herein, we demonstrated for the first time a fairly simple, straightforward, yet highly efficient method for integrating commercial electronic components onto a transparent, bendable, and stretchable substrate, by taking full advantage of our highly conductive and stretchable composite fibers. Figure 4a shows the 4 × 3 LED arrays on a transparent and stretchable substrate. The integration of the LED arrays onto the stretchable substrate was quite simple and straightforward (details in the Methods and Figure S9, Supporting Information). The prepared LED array device exhibited high transparency and was lit up at 3 V (Figure 4b from the front, Figure 4c from the back). Figure 4d demonstrates the LED arrays shining during the cyclic bending test (Supplementary Movie 2). Figure 4e shows an image

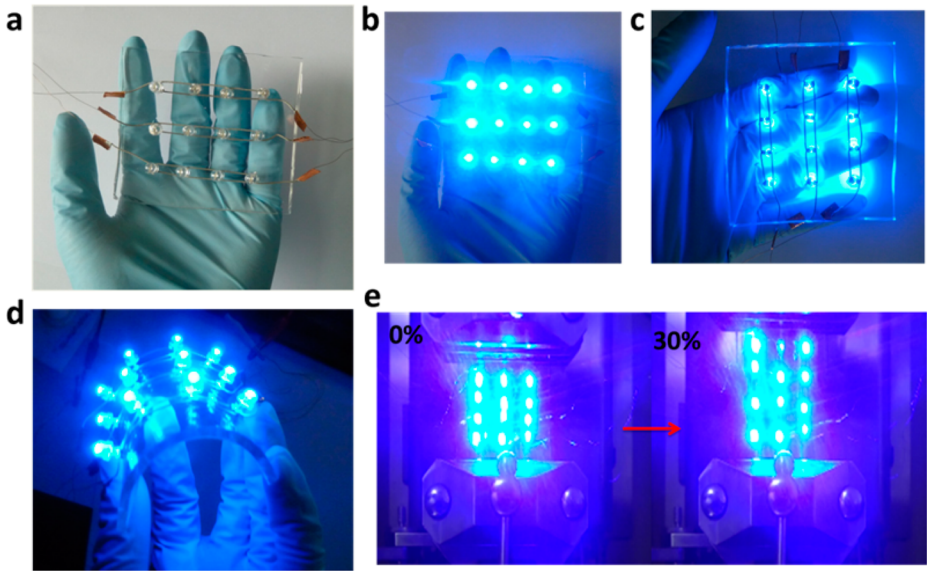

Figure 4. Transparent, bendable, and stretchable LED arrays using DCY-AgNW-PDMS in the electric circuitry. (a) Integrated LED arrays on a transparent and stretchable substrate. (b) LED arrays lit up at 3 V, from the front. (c) LED arrays lit up at 3 V, from the back. (d) LED arrays kept operational when bent; no obvious weakening of the light intensity was observed in the cyclic bending test. (e) LED arrays stayed operational when stretched to a strain of 30%.

of the shining LED arrays at 0% strain (left) and 30% strain (right). The LEDs all stayed operational (Supplementary Movie 3). These testing results successfully proved the potential application prospects of the composite fiber in large-area stretchable electronics as a robust and stretchable electrical wiring system.

Nowadays implantable devices frequently require stretchable electrical interconnects, and a critical consideration is the biocompatibility for long-term implantation in the body. To test the biocompatibility of the composite fiber, samples of DCY-AgNW-PDMS (cut into 5 mm lengths) were implanted underneath the dorsal epidermis of mice for 8 weeks. As indicated in Figure S10 (Supporting Information), no obvious inflammation was observed even after 8 weeks, verifying the biocompatibility of the composite fiber. This paves the way for its potential applications in implantable biomedical fields including human-motion detection, prosthetics, and monitoring of biosignals.

It is noteworthy that our fabrication strategy is highly versatile. For example, we can employ other nanomaterials, such as CNT and graphene, as the conducting components to obtain stretchable and conductive composite fibers with tunable performance. Furthermore, this unique "twining spring" architecture can be extended to diverse materials for the preparation of specially functionalized composite fibers with superb stretchability.

CONCLUSIONS

In summary, we have developed a novel and facile approach to fabricating highly conductive and ultrastretchable composite fibers with a unique "twining spring" configuration for stretchable electronics, which is inexpensive and already scalable for industry. The composite fiber provided high electrical conductivity even up to a strain of 500% and possessed a superb cyclic property. Its prospects in large-area stretchable electronics were demonstrated by integrating LED arrays on a transparent and stretchable substrate. We also confirmed the biocompatibility of the composite fiber to set the stage for its application in implantable biomedical devices. In addition, our fabrication strategy is versatile and can be extended to diverse materials for preparation of functionalized composite fibers.

METHODS

Fabrication of DCY-AgNW-PDMS. The double-covered yarn is widely and easily accessible in the textile market. First the DCY was cleaned in ethanol with ultrasonic treatment for about 10 min and dried in air. The DCY was then dipped into a condensed AgNW dispersion in ethanol (average length of 20 μm, average diameter of 120 nm, 20 mg/mL, from XFNANO Corporation, trace amounts of PVP in the AgNW dispersion to promote dispersibility) for 5 s and immediately dried using a blow dryer. This dip-coating process was repeated as needed to obtain AgNW-dyed yarn with varying conductivity. Then the DCY-AgNW was treated in H_2 plasma for 15 min. After that, liquid PDMS precursor (a 10:1 mixture of the PDMS prepolymer and curing agent) was dropped onto the surface of the yarn, leaving the two ends naked for electric connection. Lastly the PDMS-coated yarn was kept in a vacuum oven at 80 °C for 4 h.

Fabrication of LED Arrays Using Stretchable and Conducting Composite Fibers. A liquid PDMS precursor (a 10:1 mixture of the PDMS prepolymer and curing agent) was poured into an elastomer mold and cured at 70 °C for 10 h, obtaining a transparent and

flexible polymer substrate (8 cm × 8 cm). Then LEDs were fixed manually into the PDMS substrate in arrays of 4 × 3 by inserting the pins of LEDs into the polymer substrate (~1 mm in depth). Subsequently, fibers of DCY-AgNW (10 cm in length) were utilized as stretchable electrical wiring to integrate the LEDs in series. To enhance the electrical contact, a small amount of silver paste was smeared at the contacting position between LED pins and DCY-AgNW fibers. Lastly, a thin layer of PDMS was coated on the upper surface of the polymer substrate to fix and insulate the circuitry.

Instrumentation. Scanning electron microscopy images were taken using a Hitachi S-4800 FE-SEM. The stress *versus* strain properties were measured with a high-precision electronic universal testing machine (CMT6103, MTS Systems (China) Co., Ltd.). The stretching and bending tests of the composite fiber were also carried out on the CMT6103 universal testing machine. The four-point method is inconvenient for the real-time electrical resistance testing of the samples under mechanical deformation. Therefore, the electrical conductivity of the composite fibers was measured by a two-probe method with a FLUKE-15B digital multimeter (detailed measurement and calculation in the Supporting Information).

Conflict of Interest: The authors declare no competing financial interest.

Acknowledgment. This work was financially supported by the National Basic Research Program of China (2012CB932303), the National Natural Science Foundation of China (Grant No. 61301036), Shanghai Municipal Natural Science Foundation (Grant No. 13ZR1463600 and 13XD1403900), and The Innovation Project of Shanghai Institute of Ceramics.

Supporting Information Available: Detailed methods and complete characterization data. This material is available free of charge *via* the Internet at http://pubs.acs.org.

REFERENCES AND NOTES

1. Rogers, J. A.; Someya, T.; Huang, Y. G. Materials and Mechanics for Stretchable Electronics. *Science* **2010**, *327*, 1603–1607.
2. Kim, D. H.; Xiao, J. L.; Song, J. Z.; Huang, Y. G.; Rogers, J. A. Stretchable, Curvilinear Electronics Based on Inorganic Materials. *Adv. Mater.* **2010**, *22*, 2108–2124.
3. Gelinck, G. H.; Huitema, H. E. A.; van Veenendaal, E.; Cantatore, E.; Schrijnemakers, L.; van der Putten, J. B. P. H.; Geuns, T. C. T.; Beenhakkers, M.; Giesbers, J. B.; Huisman, B.-H.; *et al*. Flexible Active-Matrix Displays and Shift Registers Based on Solution-Processed Organic Transistors. *Nat. Mater.* **2004**, *3*, 106–110.
4. Sekitani, T.; Nakajima, H.; Maeda, H.; Fukushima, T.; Aida, T.; Hata, K.; Someya, T. Stretchable Active-Matrix Organic Light-Emitting Diode Display Using Printable Elastic Conductors. *Nat. Mater.* **2009**, *8*, 494–499.
5. Takei, K.; Takahashi, T.; Ho, J. C.; Ko, H.; Gillies, A. G.; Leu, P. W.; Fearing, R. S.; Javey, A. Nanowire Active-Matrix Circuitry for Low-Voltage Macroscale Artificial Skin. *Nat. Mater.* **2010**, *9*, 821–826.
6. Lipomi, D. J.; Vosgueritchian, M.; Tee, B. C. K.; Hellstrom, S. L.; Lee, J. A.; Fox, C. H.; Bao, Z. N. Skin-Like Pressure and Strain Sensors Based on Transparent Elastic Films of Carbon Nanotubes. *Nat. Nanotechnol.* **2011**, *6*, 788–792.
7. Yamada, T.; Hayamizu, Y.; Yamamoto, Y.; Yomogida, Y.; Izadi-Najafabadi, A.; Futaba, D. N.; Hata, K. A Stretchable Carbon Nanotube Strain Sensor for Human-Motion Detection. *Nat. Nanotechnol.* **2011**, *6*, 296–301.
8. Pang, C.; Lee, G. Y.; Kim, T. I.; Kim, S. M.; Kim, H. N.; Ahn, S. H.; Suh, K. Y. A Flexible and Highly Sensitive Strain-Gauge Sensor Using Reversible Interlocking of Nanofibres. *Nat. Mater.* **2012**, *11*, 795–801.
9. Yan, C.; Wang, J.; Kang, W.; Cui, M.; Wang, X.; Foo, C. Y.; Chee, K. J.; Lee, P. S. Highly Stretchable Piezoresistive Graphene-Nanocellulose Nanopaper for Strain Sensors. *Adv. Mater.* **2014**, *26*, 2022–2027.
10. Ko, H. C.; Stoykovich, M. P.; Song, J.; Malyarchuk, V.; Choi, W. M.; Yu, C. J.; Geddes, J. B., III; Xiao, J. L.; Wang, S. D.; Huang, Y. G.; *et al*. A Hemispherical Electronic Eye Camera Based on Compressible Silicon Optoelectronics. *Nature* **2008**, *454*, 748–753.
11. Hu, L.; Pasta, M.; Mantia, F. L.; Cui, L.; Jeong, S.; Deshazer, H. D.; Choi, J. W.; Han, S. M.; Cui, Y. Stretchable, Porous, and Conductive Energy Textiles. *Nano Lett.* **2010**, *10*, 708–714.
12. Xu, S.; Zhang, Y.; Cho, J.; Lee, J.; Huang, X.; Jia, L.; Fan, J. A.; Su, Y. W.; Su, J.; Zhang, H. G. Stretchable Batteries with Self-Similar Serpentine Interconnects and Integrated Wireless Recharging Systems. *Nat. Commun.* **2013**, *4*, 1543.
13. Jeong, G. S.; Baek, D. H.; Jung, H. C.; Song, J. H.; Moon, J. H.; Hong, S. W.; Kim, I. Y.; Lee, S. H. Solderable and Electroplatable Flexible Electronic Circuit on a Porous Stretchable Elastomer. *Nat. Commun.* **2012**, *3*, 977.
14. Kim, Y.; Zhu, J.; Yeom, B.; Di Prima, M.; Su, X.; Kim, J. G.; Yoo, S. J.; Uher, C.; Kotov, N. A. Stretchable Nanoparticle Conductors with Self-Organized Conductive Pathways. *Nature* **2013**, *500*, 59–63.
15. Kujawski, M.; Pearse, J. D.; Smela, E. Elastomers Filled with Exfoliated Graphite as Compliant Electrodes. *Carbon* **2010**, *48*, 2409–2417.
16. Sekitani, T.; Noguchi, Y.; Hata, K.; Fukushima, T.; Aida, T.; Someya, T. A Rubberlike Stretchable Active Matrix Using Elastic Conductors. *Science* **2008**, *321*, 1468–1472.
17. Chun, K.-Y.; Oh, Y.; Rho, J.; Ahn, J.-H.; Kim, Y.-J.; Choi, H. R.; Baik, S. Highly Conductive, Printable and Stretchable Composite Films of Carbon Nanotubes and Silver. *Nat. Nanotechnol.* **2010**, *5*, 853–857.
18. Hansen, T. S.; West, K.; Hassager, O.; Larsen, N. B. Highly Stretchable and Conductive Polymer Material Made from Poly (3, 4-ethylenedioxythiophene) and Polyurethane Elastomers. *Adv. Funct. Mater.* **2007**, *17*, 3069–3073.
19. Shin, M. K.; Oh, J.; Lima, M.; Kozlov, M. E.; Kim, S. J.; Baughman, R. H. Elastomeric Conductive Composites Based on Carbon Nanotube Forests. *Adv. Mater.* **2010**, *22*, 2663–2667.
20. Kim, K. H.; Vural, M.; Islam, M. F. Single-Walled Carbon Nanotube Aerogel-Based Elastic Conductors. *Adv. Mater.* **2011**, *23*, 2865–2869.
21. Chen, Z.; Ren, W.; Gao, L.; Liu, B.; Pei, S.; Cheng, H.-M. Three Dimensional Flexible and Conductive Interconnected Graphene Networks Grown by Chemical Vapour Deposition. *Nat. Mater.* **2011**, *10*, 424–428.
22. Khang, D.-Y.; Xiao, J.; Kocabas, C.; MacLaren, S.; Banks, T.; Jiang, H.; Huang, Y. Y.; Roger, J. A. Molecular Scale Buckling Mechanics in Individual Aligned Single-Wall Carbon Nanotubes on Elastomeric Substrates. *Nano Lett.* **2008**, *8*, 124–130.
23. Xiao, J.; Carlson, A.; Liu, Z. J.; Huang, Y.; Jiang, H.; Rogers, J. A. Stretchable and Compressible Thin Films of Stiff Materials on Compliant Wavy Substrates. *Appl. Phys. Lett.* **2008**, *93*, 013109.
24. Zu, M.; Li, Q.; Wang, G.; Byun, J. H.; Chou, T. W. Carbon Nanotube Fiber Based Stretchable Conductor. *Adv. Funct. Mater.* **2013**, *23*, 789–793.
25. Liu, K.; Sun, Y.; Liu, P.; Lin, X.; Fan, S.; Jiang, K. Cross-Stacked Superaligned Carbon Nanotube Films for Transparent and Stretchable Conductors. *Adv. Funct. Mater.* **2011**, *21*, 2721–2728.
26. Li, T.; Huang, Z.; Suo, Z.; Lacour, S. P.; Wagner, S. Stretchability of Thin Metal Films on Elastomer Substrates. *Appl. Phys. Lett.* **2004**, *85*, 3435–3437.
27. Cai, L.; Li, J.; Luan, P.; Dong, H.; Zhao, D.; Zhang, Q.; Zhang, X.; Tu, M.; Zeng, Q. S.; Zhou, W. Y. Highly Transparent and Conductive Stretchable Conductors Based on Hierarchical Reticulate Single-Walled Carbon Nanotube Architecture. *Adv. Funct. Mater.* **2012**, *22*, 5238–5244.
28. Zhu, Y.; Xu, F. Buckling of Aligned Carbon Nanotubes as Stretchable Conductors: A New Manufacturing Strategy. *Adv. Mater.* **2012**, *24*, 1073–1077.
29. Zhang, Y.; Sheehan, C. J.; Zhai, J.; Zou, G.; Luo, H.; Xiong, J.; Zhu, Y. T.; Jia, Q. X. Polymer-Embedded Carbon Nanotube Ribbons for Stretchable Conductors. *Adv. Mater.* **2010**, *22*, 3027–3031.

30. Xu, F.; Zhu, Y. Highly Conductive and Stretchable Silver Nanowire Conductors. *Adv. Mater.* **2012**, *24*, 5117–5122.
31. Wang, X.; Hu, H.; Shen, Y.; Zhou, X.; Zheng, Z. Stretchable Conductors with Ultrahigh Tensile Srain and Stable Metallic Conductance Enabled by Prestrained Polyelectrolyte Nanoplatforms. *Adv. Mater.* **2011**, *23*, 3090–3094.
32. Béfahy, S.; Yunus, S.; Pardoen, T.; Bertrand, P.; Troosters, M. Stretchable Helical Gold Conductor on Silicone Rubber Microwire. *Appl. Phys. Lett.* **2007**, *91*, 141911.
33. Lacour, S. P.; Jones, J.; Wagner, S.; Li, T.; Suo, Z. Stretchable Interconnects for Elastic Electronic Surfaces. *Proc. IEEE* **2005**, *93*, 1459–1467.
34. Lee, P.; Lee, J.; Lee, H.; Yeo, J.; Hong, S.; Nam, K. H.; Lee, D. J.; Lee, S. S.; Ko, S. H. Highly Stretchable and Highly Conductive Metal Electrode by Very Long Metal Nanowire Percolation Network. *Adv. Mater.* **2012**, *24*, 3326–3332.
35. Xu, Z.; Liu, Z.; Sun, H.; Gao, C. Highly Electrically Conductive Ag-Doped Graphene Fibers as Stretchable Conductors. *Adv. Mater.* **2013**, *25*, 3249–3253.
36. Wu, J.; Ashraf, S. A.; Wallace, G. G. Conducting Textiles from Single-Walled Carbon Nanotubes. *Synth. Met.* **2007**, *157*, 358–362.
37. Liu, X.; Chang, H.; Li, Y.; Huck, W. T.; Zheng, Z. Polyelectrolyte-Bridged Metal/Cotton Hierarchical Structures for Highly Durable Conductive Yarns. *ACS Appl. Mater. Interfaces* **2010**, *2*, 529–535.
38. Kang, T. J.; Choi, A.; Kim, D. H.; Jin, K.; Seo, D. K.; Jeong, D. H.; Hong, S.-H.; Park, Y. W.; Kim, Y. H. Electromechanical Properties of CNT-Coated Cotton Yarn for Electronic Textile Applications. *Smart Mater. Struct.* **2011**, *20*, 015004.
39. Yun, Y. J.; Hong, W. G.; Kim, W. J.; Jun, Y.; Kim, B. H. A Novel Method for Applying Reduced Graphene Oxide Directly to Electronic Textiles from Yarns to Fabrics. *Adv. Mater.* **2013**, *25*, 5701–5705.
40. Zhang, D.; Wang, R.; Wen, M.; Weng, D.; Cui, X.; Sun, J.; Li, H. X.; Lu, Y. Synthesis of Ultralong Copper Nanowires for High-Performance Transparent Electrodes. *J. Am. Chem. Soc.* **2012**, *134*, 14283–14286.
41. Wang, R.; Chen, Z.; Yu, H.; Jia, X.; Gao, L.; Sun, J.; Hicks, R. F.; Lu, Y. A Novel Method to Enhance the Conductance of Transitional Metal Oxide Electrodes. *Nanoscale* **2014**, *6*, 3791–3795.
42. Park, M.; Im, J.; Shin, M.; Min, Y.; Park, J.; Cho, H.; Park, S.; Shim, M. B.; Jeon, S.; Chung, D. Y.; *et al*. Highly Stretchable Electric Circuits from a Composite Material of Silver Nanoparticles and Elastomeric Fibres. *Nat. Nanotechnol.* **2012**, *7*, 803–809.
43. Ge, J.; Yao, H.-B.; Wang, X.; Ye, Y.-D.; Wang, J.-L.; Wu, Z.-Y.; Liu, J.-W.; Fan, F.-J.; Gao, H.-L.; Zhang, C.-L.; *et al*. Stretchable Conductors Based on Silver Nanowires: Improved Performance through a Binary Network Design. *Angew. Chem., Int. Ed.* **2013**, *125*, 1698–1703.
44. Yu, Y.; Zeng, J.; Chen, C.; Xie, Z.; Guo, R.; Liu, Z.; Zhou, X. C.; Yang, Y.; Zheng, Z. Three-Dimensional Compressible and Stretchable Conductive Composites. *Adv. Mater.* **2014**, *26*, 810–815.
45. Park, J.; Wang, S.; Li, M.; Ahn, C.; Hyun, J. K.; Kim, D. S.; Kim, D. K.; Rogers, J. A.; Huang, Y. G.; Jeon, S. Three-Dimensional Nanonetworks for Giant Stretchability in Dielectrics and Conductors. *Nat. Commun.* **2012**, *3*, 916.